

A Combined Pressure-controlled Scanning Calorimetry and Monte Carlo Determination of the Joule–Thomson Inversion Curve. Application to Methane

D. Bessières,^{*,†} S. L. Randzio,[‡] M. M. Piñeiro,[§] Th. Lafitte,[†] and J-L. Daridon[†]

Laboratoire des Fluides Complexes, UMR 5150, Université de Pau, Avenue de l'Université, B.P. 11 55, 64013 PAU Cedex, France, Polish Academy of Science, Institute of Physical Chemistry, ul. Kasprzaka 44/52, 01–224 Warszawa, Poland, and Departamento de Física Aplicada, Faculdade de Ciencias, Universidade de Vigo, E36310 Vigo, Spain

Received: December 3, 2005; In Final Form: January 27, 2006

A combination of a pressure-controlled scanning calorimetry (PCSC) and Monte Carlo simulations (MCS) is presented for an unequivocal determination of the Joule–Thomson inversion curve (JTIC) with high accuracy over wide ranges of pressure and temperature. The MCS performed with the fluctuation method are fast and easy to operate, but the results can vary significantly depend on the set of primary molecular data needed for the calculations. The PCSC is an experimental and more laborious technique, but supplies data of high quality. Thus, it can be used to check the MCS data and to verify the molecular parameters used for the calculations. Such a combined procedure was used in the present study for determination of the JTIC for methane, for which a correlation equation was established valid from 302.9 to 586.5 K. A combination of a direct experimental technique with molecular simulations permits also to better understand the complex behavior of the Joule–Thomson inversion phenomenon over wide ranges of pressure and temperature.

Introduction

When a fluid moving along a pipeline finds a sudden narrowing, e.g., a valve, a process known as Joule–Thomson expansion (or throttling) takes place. An important feature of such a process is that the enthalpy of the fluid remains constant and the temperature may either increase, decrease, or remain constant depending on pressure and temperature conditions. A significant information on such a process can be obtained from the so-called Joule–Thomson coefficient μ_{JT} (JTC), especially when it is known over wide pressure and temperature ranges¹

$$\mu_{JT} = \left(\frac{\partial T}{\partial P} \right)_H \quad (1)$$

The JTC can vary from positive to negative values. The locus of points where the JTC equals zero

$$\mu_{JT} = 0 \quad (2)$$

is called the Joule–Thomson inversion curve (JTIC), which in the (P, T) plane separates regions where cooling or heating occur due to the throttled gas expansion. The throttling has a remarkable relevance in various industries, for example, in cryogenic processes, where it is frequently used for cooling or liquefaction of gases. Another practical application of JTIC has arisen recently in reservoir engineering. The urgent need to find new sources of natural gas and oil, together with the latest improvements in drilling technologies, have led to deeper prospective explorations either inland or off-shore, where temperatures up to 520 K and pressures up to 120 MPa can be reached. As a result, when gas condensates are pumped out of

high pressures reservoirs, the inversion phenomena may occur and cause an unexpected temperature change of the gas condensates. Such changes can affect and damage surface production operations. Thus, the accurate characterization of this abnormal behavior (e.g., heating effect resulting from an expansion), plays an essential role in their technical design, operation, and maintenance of such processes. For the above reasons, the accurate determination of JTIC is of great importance in many practical applications.

Such practical applications and their consequences were the starting point of numerous studies of the JTIC phenomenon. A large number of them have been based on using equations of state (EOS). The condition for existence of the inversion curve, defined by eq 2, can be transformed into eq 3 which is the most

$$T \left(\frac{\partial P}{\partial T} \right)_V + V \left(\frac{\partial P}{\partial V} \right)_T = 0 \quad (3)$$

direct thermodynamic basis for the calculation of the JTIC with an EOS. Chacin et al.² have reviewed the use of cubic EOS for the JTIC estimation. They concluded that such a task largely exceeds the applicability limit of the commonly used cubic equations, which have been mainly developed and tuned for classic phase equilibria estimations. More recent studies are concerned with equations of states based on molecular models. Colina et al. have published predictions for the JTIC for *n*-alkanes³ and carbon dioxide⁴ with the use of SAFT EOS in its soft-version. The main advantage of this approach is that the molecular parameters have sound and well established physical meanings and are valid over wide pressure and temperature ranges. However, the authors conclude that the determination of the inversion curve is a severe test for this approach and that the final results strongly depend on the set of parameters used. The situation could be improved, if precise experimental data existed for the verification of the calculated inversion curve.

* Corresponding author e-mail: david.bessieres@univ-pau.fr.

[†] Université de Pau.

[‡] Polish Academy of Science.

[§] Universidade de Vigo.

However, direct experimental measurement of the inversion points was, up to now, very difficult and highly unreliable. A feasible operating procedure could consist of producing a throttling expansion in a flow calorimeter. A shortcoming for this technique is that the combined appropriate use of both flow rate and pressure cannot be obtained with a sufficient precision at pressures exceeding 30 MPa.⁵ Besides this instrumental limitation, the fundamental reason to refuse this method remains in the JTC value itself. Near the inversion zone, the vanishing JTC values imply that even large pressure differences lead to very small thermal effects, which, unfortunately, cannot be detected with reliable accuracy. An alternative route is provided via thermodynamic relations. The JTC can be expressed in terms of available fluid parameters¹

$$\mu_{JT} = \frac{V_m}{C_{p,m}}(\alpha T - 1) = \frac{RT^2}{PC_{p,m}}\left(\frac{\partial Z}{\partial T}\right)_P \quad (4)$$

where V_m is the molar volume, $C_{p,m}$ is the molar isobaric heat capacity, α is cubic expansion coefficient, and Z is the compressibility factor. One can see from eq 4 that the inversion curve is obtained by satisfying the conditions for which the JTC equals zero:

$$\alpha T - 1 = 0 \quad (5)$$

or

$$\left(\frac{\partial Z}{\partial T}\right)_P = 0 \quad (6)$$

With the use of a pressure-controlled scanning calorimeter (PCSC) adapted previously to measurements of thermal expansion of dense gases,⁶ pressure and temperature coordinates can be precisely measured, where the condition defined by eq 5 is fully satisfied.

On the other hand recent developments of the Monte Carlo technique permit us to determine pressure and temperature coordinates of the points in the (P , T) plane, where the conditions defined by either eq 4 or eq 5 or both are satisfied. Colina and Muller^{7,8}, using Monte Carlo molecular simulation in the NPT (isothermal isobaric) ensemble, demonstrated a possibility of accurate determination of the behavior of the compressibility factor Z along different isobars and then, using the condition defined by eq 5, could determine the locus of points creating the JTIC. The method can be successively applied to Lennard–Jones molecular liquids, but also for molecules involving Coulombic or polar interactions, e.g., CO_2 , as shown recently by Colina et al.⁹ Alternatively, Lagache et al.¹⁰ applied NPT Monte Carlo simulation to compute second-order derivatives of the Gibbs energy from the energy and volume statistical fluctuations along a simulation run and demonstrated that this approach is reliable for estimation of thermal expansion, isothermal compressibility, isobaric and isochoric heat capacities (provided that an ideal gas term correlation is available), speed of sound, and JT coefficient over wide pressure and temperature ranges. The method was applied with good results to pure short alkanes and their mixtures in the original work, and later extended to a complex mixture reproducing a natural gas condensate.¹¹ Colina et al.¹² have also applied such a method to CO_2 derivative property estimation. Thus, determination of thermal expansion coefficient can be used for the JTIC determination with the use of the condition defined by eq 4. However, both Monte Carlo approaches, summarized by Ungerer et al.¹³, require a reliable parametrization of intermolecular and intramolecular potentials of the system under investigation and

thus must be verified in one or another way. Lisal et al.¹⁴ applied a different simulation technique to study the JT expansion, based on the constant enthalpy and pressure MC method, which allows direct calculation of the temperature change. Escobedo and Chen¹⁵ estimated the JT inversion phenomena by evaluation of alternatives for simulation of isobars and isotherms, thermodynamic integration, and histogram reweighing techniques.

As it was mentioned above, the experimental PCSC technique can be used as a direct, safe, and reliable experimental method for the determination of the inversion curve, based on the condition defined by eq 5. However, the technique is rather laborious and time-consuming in an attempt to determine precisely the whole inversion curve. On the other hand, the Monte Carlo molecular simulations are much faster, but their results can depend on the set of primary data needed for the calculations, thus they need to be verified. For this reason it is proposed in the present study to combine both techniques. The rather easily determined Monte Carlo data for the inversion curve could be experimentally verified in selected regions by the PCSC technique, and thus the final results would be reliable and rather easily obtained. The use of such a combined approach will be illustrated with determination of the Joule–Thomson inversion curve for methane, which is a major component in the gas condensates and plays an important role in oil and gas industries.

Techniques

Pressure-Controlled Scanning Calorimetry. Measurement and calibration procedures for PCSC determination of thermal expansion of gases over wide pressure and temperature ranges have been described previously.⁶ Thus, at the present contribution only a short recall is given. The thermodynamic basis for the direct determination of α is the following Maxwell relation:

$$\left(\frac{\partial V_m}{\partial T}\right)_P = \left(\frac{\partial S_m}{\partial P}\right)_T = -\frac{1}{T}\left(\frac{\partial Q_m}{\partial P}\right)_T = \alpha V_m \quad (7)$$

In a calorimeter with a mass open calorimetric vessel having the active volume V_E (in cm^3) and a calorimetric detector having the sensibility k (in mW/mV) relation (7) can be transformed into the following form:

$$\alpha = -\frac{k}{V_E} \frac{I}{T\Delta P} + \alpha_{ss} \quad (8)$$

where I (in Vs) is the integral of the calorimetric detector response to the pressure change ΔP (in MPa), T is temperature (in K), and α_{ss} is the cubic thermal expansion of stainless steel from which the calorimetric vessel was made ($5 \times 10^{-5} \text{ K}^{-1}$). Pressure changes $\Delta P = 2 \text{ MPa}$ have been performed with an automated pump at a controlled rate of 0.016 MPa s^{-1} , which was sufficient to ensure equilibrated heat exchange between the gas, calorimetric vessel, and the calorimetric detector under quasi-isothermal conditions, required by the Maxwell relation (7). The ratio of the calibration constants k/V_E and its dependence on temperature was determined on the basis of both gas expansion and heat capacity of calibrating fluids. As it was previously demonstrated, its pressure dependence is negligible.⁶ In the present study, the set of results obtained at each selected temperature was fitted to a function $\alpha T = f(P)$. With a careful analysis of the fitted curve the pressure was determined, where $\alpha T = 1$. Performing measurements at various selected temperatures a set of (P , T) coordinates could be obtained, where $\alpha T = 1$ and thus to define precisely the locus of points which create

TABLE 1: Experimental Data of the Volume Expansion Coefficient, α , Obtained with Pressure-controlled Scanning Calorimetry over the Pressure Range from 15 to 80 MPa at Selected Temperatures from 302.9 to 511.7 K

p/MPa	$\alpha/10^{-3} \text{ K}^{-1}$	$\Delta\alpha/10^{-5} \text{ K}^{-1}$	p/MPa	$\alpha/10^{-3} \text{ K}^{-1}$	$\Delta\alpha/10^{-5} \text{ K}^{-1}$	p/MPa	$\alpha/10^{-3} \text{ K}^{-1}$	$\Delta\alpha/10^{-5} \text{ K}^{-1}$	p/MPa	$\alpha/10^{-3} \text{ K}^{-1}$	$\Delta\alpha/10^{-5} \text{ K}^{-1}$
T = 302.9 \pm 0.2 K						T = 402.4 \pm 0.2 K					
59.9	2.47	7	47.9	3.14	9	60.0	2.36	7	48.1	2.65	8
57.9	2.63	7	46.0	3.31	9	56.1	2.42	7	46.2	2.71	8
55.9	2.73	8	44.0	3.45	10	54.1	2.46	7	44.1	2.79	8
53.9	2.77	8	42.0	3.57	10	52.1	2.52	7	42.1	2.87	8
51.9	2.86	8	40.0	3.73	10	50.1	2.56	7	40.1	2.96	8
49.9	2.99	8									
T = 312. \pm 0.2 K						T = 412.3 \pm 0.2 K					
61.9	2.42	7	50.0	3.00	8	61.9	2.21	6	51.9	2.49	7
59.9	2.52	7	48.0	3.13	9	59.9	2.26	6	48.0	2.59	7
57.9	2.61	7	46.0	3.26	9	58.0	2.33	7	44.0	2.66	8
55.9	2.69	8	44.0	3.39	10	56.0	2.39	7	42.0	2.72	8
53.9	2.79	8	42.0	3.52	10	53.9	2.38	7	39.9	2.77	8
51.9	2.91	8	40.0	3.69	10						
T = 322.8 \pm 0.2 K						T = 422.3 \pm 0.2 K					
69.8	2.25	6	48.0	3.13	9	79.7	1.93	6	48.7	2.49	7
62.0	2.49	7	46.0	3.24	9	69.8	2.05	6	44.7	2.59	7
60.0	2.59	7	44.0	3.34	9	57.9	2.28	7	42.7	2.64	8
58.0	2.65	8	42.0	3.48	10	54.0	2.37	7	29.8	2.88	8
56.0	2.71	8	40.0	3.63	10	52.0	2.41	7	20.0	2.99	8
54.0	2.80	8	29.9	4.45	10	50.0	2.45	7	15.0	2.95	8
52.0	2.89	8	20.0	5.40	10						
50.0	3.04	9	15.0	5.29	10						
T = 332.8 \pm 0.2 K						T = 432.1 \pm 0.2 K					
61.9	2.46	7	50.0	2.98	8	61.9	2.12	6		2.41	7
60.0	2.56	7	48.0	3.08	9	59.9	2.16	6		2.47	7
58.0	2.64	8	46.0	3.19	9	58.0	2.21	6		2.55	7
56.0	2.73	8	44.0	3.26	9	56.0	2.26	6		2.60	7
54.0	2.80	8	42.0	3.4	10	54.0	2.30	7		2.67	8
52.0	2.89	8	40.0	3.5	10	52.0	2.38	7		2.73	8
T = 342.7 \pm 0.2 K						T = 442.1 \pm 0.2 K					
61.9	2.41	7	50.0	2.96	8	60.0	2.14	6	46.0	2.46	7
59.9	2.48	7	48.0	3.04	9	58.0	2.18	6	44.0	2.50	7
58.0	2.58	7	46.0	3.08	9	54.0	2.26	6	42.0	2.56	7
56.0	2.67	8	43.9	3.17	9	50.0	2.35	7	40.0	2.62	7
54.0	2.75	8	42.0	3.31	9	48.0	2.40	7			7
52.0	2.81	8	39.9	3.37	9						
T = 352.6 \pm 0.2 K						T = 452.1 \pm 0.2 K					
62.0	2.43	7	50.0	2.96	8	61.9	2.01	6	50.0	2.30	7
60.0	2.50	7	48.0	3.04	8	59.9	2.07	6	48.0	2.34	7
58.0	2.57	7	46.0	3.08	9	58.0	2.12	6	46.0	2.39	7
56.0	2.64	8	43.9	3.17	9	55.9	2.14	6	43.9	2.44	7
54.0	2.73	8	42.0	3.31	9	53.9	2.21	6	42.0	2.50	7
52.0	2.81	8	40.0	3.37	10	52	2.24	6	40.0	2.52	7
T = 372.6 \pm 0.2 K						T = 462.0 \pm 0.2 K					
79.7	1.98	6	50.0	2.76	8	61.9	2.02	6	51.9	2.21	6
77.7	2.02	6	48.0	2.84	8	60.0	2.05	6	47.9	2.27	7
71.8	2.11	6	46.0	2.93	8	58.0	2.09	6	41.9	2.39	7
69.8	2.15	6	44.0	3.01	8	56.0	2.12	6	40.0	2.43	7
59.9	2.38	7	42.0	3.12	9	53.9	2.14	6			
57.9	2.46	7	40.0	3.19	9						
55.9	2.53	7	30.0	3.50	10						
53.9	2.61	7	20.0	3.80	10						
51.9	2.69	7	15.0	3.70	10						
T = 382.5 \pm 0.2 K						T = 471.9 \pm 0.2 K					
57.7	2.45	7	45.7	2.88	8	62.0	1.97	6	46.0	2.25	6
53.7	2.58	7	43.6	2.96	8	57.9	2.04	6	44.0	2.28	7
51.7	2.65	8	41.7	3.05	9	56.0	2.08	6	42.0	2.32	7
47.7	2.80	8				54.0	2.11	6			
T = 392.5 \pm 0.2 K						T = 491.8 \pm 0.2 K					
59.9	2.34	7	47.9	2.73	8	59.9	1.96	6	47.9	2.09	6
58.0	2.40	7	45.9	2.79	8	57.9	1.98	6	45.9	2.11	6
55.9	2.47	7	43.9	2.88	8	49.9	2.07	6	40.0	2.18	6
53.9	2.52	7	41.9	2.92	8						
51.9	2.59	7	40.0	3.03	9						
49.9	2.65	8									
T = 511.7 \pm 0.2 K											
						57.9	1.87	5	50.0	1.98	6
						55.9	1.90	5	47.9	2.00	6
						54.0	1.92	6	42.0	2.08	6

the Joule–Thomson inversion curve for the system under investigation.

Monte Carlo Molecular Simulations. Monte Carlo calculations were organized as follows: 500 molecules were placed in a cubic box where the usual periodic boundary conditions

and minimum image conventions were applied. The molecules were placed at first in a cubic lattice. Interaction between methane molecules was described through an united atom Lennard–Jones potential, parametrized according to Möller et al.¹⁶ A constant cut off radius of 14 Å was used, together with

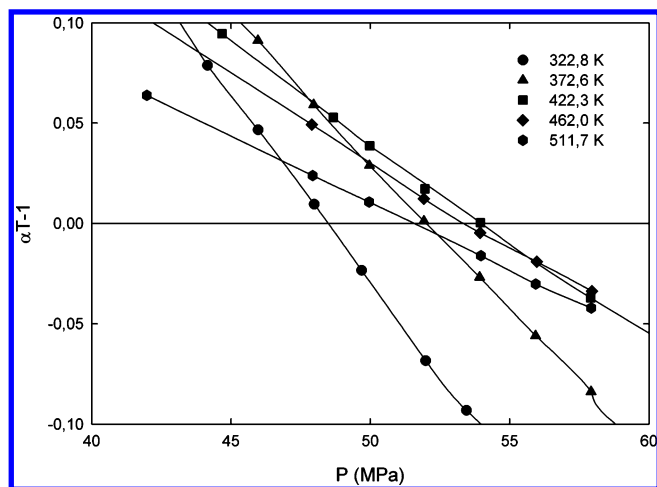


Figure 1. An example of determination of the coordinates of the Joule–Thomson inversion curve (JTIC) for methane from the pressure-controlled scanning calorimetry data presented in Table 1.

the corresponding potential tail correction. Block average was used to estimate uncertainties along the simulations. The simulation was divided in cycles, each one consisting of 500 attempts to displace a molecule and one attempt to change volume. The amplitudes of displacement and volume changes were adjusted along each run to achieve an acceptance probability of 50% in both cases. A complete simulation run consisted typically of 2×10^5 equilibration cycles followed by 6×10^5 production cycles. Details about NPT Monte Carlo simulations can be found elsewhere.^{17,18}

Materials

Methane was from Messer, 99.999% purity and used without further treatment.

PCSC Results. Volume expansion coefficient, α , for methane was measured with a PCSC over the pressure range from 40 to 60 MPa and over the temperature range from 302.9 to 511.7 K, where the inversion phenomenon may occur. The results of the measurements are given in Table 1. As it was analyzed previously,¹⁹ the expected precision in PCSC determination of α for compressed fluids is about 2.7% based in the uncertainties in the measured pressure ± 0.15 MPa; reproducibility of the calorimetric signal $\pm 1\%$, temperature, ± 0.2 K; the calibration constant 0.7%; and $\pm \alpha_{SS}$ 10%.

Along the isothermal curves, the quantities $(\alpha T - 1)$, generated from the thermal expansion data, were fitted with a polynomial. The inversion pressures corresponding to the temperatures considered were deduced from relation (5) by intersection of the polynomial form with the pressure axis. An example of such a procedure for several temperatures is given in Figure 1. The linear dependence of $(\alpha T - 1)$ on pressure, obtained in the whole temperature range near the inversion curve induces small errors on the pressure dependence. A statistical analysis shows that random or non random errors generated on volume expansion data on the inversion curve cause an uncertainty inferior to 0.3 MPa. A collection of all determined (P, T) coordinates for the inversion curve for methane is given in Table 2. To the best of our knowledge, this is the most direct experimental data on the Joule–Thomson inversion curve obtained up to date. A comparison of the present experimental data with the data derived from the literature is given in Figure 2. The following literature sources have been taken for the comparison: a general correlation for the JTIC proposed by Gunn et al.,²⁰ data from IUPAC recommended volumetric properties^{21,22} derived with

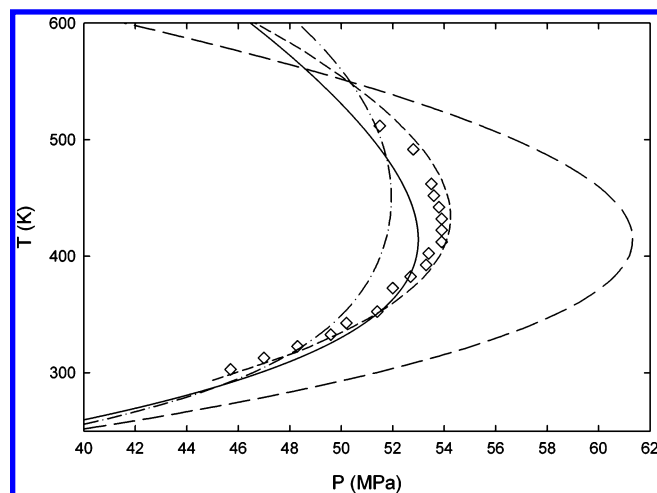


Figure 2. Comparison of results obtained in the present study for the Joule–Thomson inversion curve (JTIC) for methane: experimental (\diamond); (—) Gunn et al.²⁰ correlation; (---) derived from IUPAC recommended data; (- - -) PC-SAFT predicted, and (—) VR-SAFT predicted.

TABLE 2: (P,T) Locus of the Joule–Thomson Inversion Curve for Methane Obtained from PCSC Data Presented in Table 1

p_{JTIC}/MPa	T_{JTIC}/K	p_{JTIC}/MPa	T_{JTIC}/K
45.7	302.9	53.9	412.3
47.0	312.8	53.9	422.3
48.3	322.8	53.9	432.1
49.6	332.7	53.8	442.1
50.2	342.7	53.6	452.1
51.4	352.6	53.5	462.0
52.0	372.6	52.8	491.8
52.7	382.5	51.5	511.7
53.3	392.5		
53.4	402.4		

the use of criteria (5) and (6), and data from the SAFT EOS,²³ the most popular molecular equation of state in use today, especially in the versions PC-SAFT²⁴ and VR-SAFT,²⁴ derived with the use of criterion (6). One can see that the present experimental results exhibit a very good agreement with the data derived from the IUPAC recommended volumetric properties.

Monte Carlo Results. Simulations were performed for isobars from 40 to 53.5 MPa at temperatures from 200 to 700 K, completing a total of 90 simulation points. Derived properties were calculated with the fluctuation method.¹⁰ The accuracy of the simulation method based on the density determination was 0.78 average percent deviation (APD) with respect to the recommended literature values.²¹ On the basis of the results of such calculations the JT inversion points were obtained using both criteria described above (eqs 5 and 6). The method based on criterion (6) was more accurate to identify JT inversion points over the whole (P, T) range than the method based on the criterion related to volume expansion coefficient (eq 5), due to the difference in propagation of statistical errors. In Figure 3 an example is given of calculations at 46 MPa, which shows that the compressibility factor data were obtained with low statistical scattering, this allows accurate identification of the inversion phenomena through proper interpolation. As for the uncertainties in compressibility factor determination, the block average method along a simulation run yielded typical percent deviation values below 0.12%. For a given isobar, the influence of this compressibility factor fluctuation on the given inversion point coordinates must be evaluated, through an analysis of the interpolation performed to identify the maximum and minimum

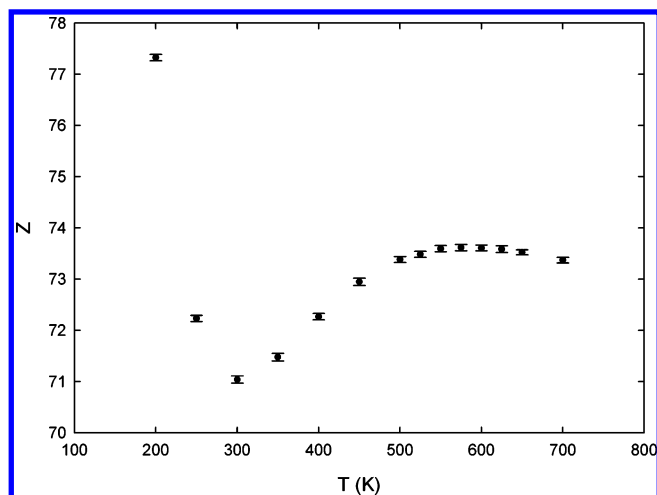


Figure 3. Compressibility factor (Z) for methane obtained with the Monte Carlo simulations at 46 MPa, together with the corresponding error bar for each point.

TABLE 3: (P, T) Locus of the Joule–Thomson Inversion Curve for Methane Determined with the NPT Monte Carlo Simulations

p_{JTIC}/MPa	T_{JTIC}/K	p_{JTIC}/MPa	T_{JTIC}/K
46.0	302	53.5	447
48.0	321	53.0	478
49.0	327	52.0	509
50.0	340	51.0	524
51.0	352	50.0	540
52.0	367	49.0	565
53.0	387	48.0	571
53.5	398	46.0	587

in the Z vs T representation. This uncertainty in inversion temperature determination (due only to the interpolation method), has been calculated numerically to be lower than 2 K. The whole set of inversion points calculated with Monte Carlo simulations is given in Table 3. One should notice that the MCS data have reasonable values beyond the interval where the experimental data were collected. This result is highly encouraging, because it proves that the determination of the JTIC with the MC simulations is more accurate than any other known theoretical approach.

Combined Correlation Equation for the JTIC for Methane. Both the experimental data from Table 2 obtained with the pressure-controlled scanning calorimetry and the data from Table 3 obtained with the Monte Carlo simulations have been fitted to a correlation equation

$$P_r = -31.996 + 59.453T_r - 30.489T_r^2 + 7.1824T_r^3 - 0.68542T_r^4 \quad (9)$$

where $P_r = (P/P_c)$ is the reduced pressure, and $T_r = (T/T_c)$ is the reduced temperature of methane for which $P_c = 4.61$ MPa and $T_c = 190.6$ K. Eq (9) represents the Joule–Thomson inversion curve for methane over the temperature range from 302.9 to 586.5 K with a mean deviation of 0.34% (or 0.17 MPa) from all data, both experimental and simulated. Figure 4 presents on the (P, T) surface both the PCSC experimental data and the NPT MCS calculated data together with the JTIC established with eq 9.

Conclusion

It was demonstrated that exact data for the Joule–Thomson inversion curve can be experimentally determined with the use

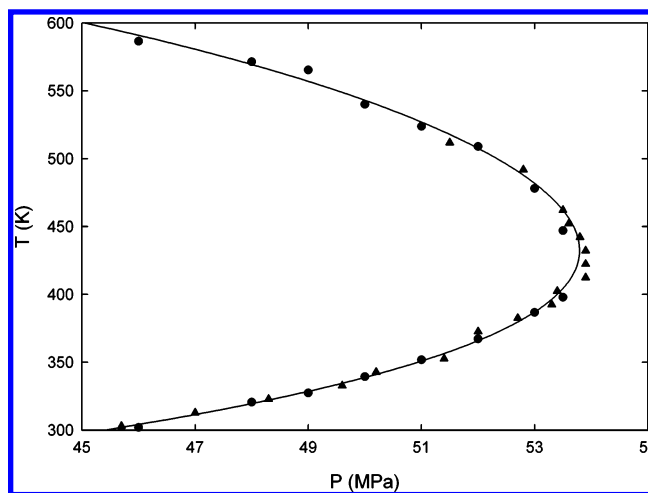


Figure 4. Comparison of results obtained in the present study for the Joule–Thomson inversion curve for methane: experimental PCSC (▲), determined with Monte Carlo simulations (●) and eq 9 (line).

of pressure-controlled scanning calorimetry. On the other hand the Joule–Thomson inversion curve can be determined much faster and easier with the use of Monte Carlo simulations, but the simulation results depend on the molecular parameters used for the calculations. The PCSC data can be used to check the MCS data at selected regions of pressure and temperature and to verify the molecular parameters taken for the calculations. Such a combined procedure was used in the present study for determination of the Joule–Thomson inversion curve for methane, for which a correlation equation was established valid from 302.9 to 586.5 K with a mean deviation of 0.34% (or 0.17 MPa) from all the data, both experimental and simulated. A combination of a direct experimental technique with molecular simulations permits also to better understand the complex behavior of the Joule–Thomson inversion phenomenon over wide ranges of pressure and temperature.

Acknowledgment. M. M. P. acknowledges CESGA (Santiago de Compostela, Spain) for providing access to computing facilities.

References and Notes

- (1) Reif, F. *Fundamentals of Statistical and Thermal Physics*, 1st ed.; McGraw-Hill: New York, 1965; pp 178–184.
- (2) Chacín, A.; Vázquez, J. M.; Müller, E. A. *Fluid Phase Equilib.* **1999**, *165*, 147–155.
- (3) Colina, C.; Turens, L. F.; Gubbins, K. E.; Olivera-Fuentes, C.; Vega, L. F. *Ind. Eng. Chem. Res.* **2002**, *41*, 1069–1075.
- (4) Colina, C.; Olivera-Fuentes, C. *Ind. Eng. Chem. Res.* **2002**, *41*, 1064–1068.
- (5) Grini, P.; Owren, G. O. A.; Maelhum, H. J. *Chem. Therm.* **1998**, *30*, 1011–1027.
- (6) Bessières, D.; Lafitte, Th.; Daridon, J.-L.; Randzio, S. L. *Thermochim. Acta* **2005**, *428*, 25–30.
- (7) Colina, C.; Müller, E. A. *Mol. Sim.* **1997**, *19*, 273–286.
- (8) Colina, C.; Müller, E. A. *Int. J. Thermophys.* **1999**, *20* (1), 229–235.
- (9) Colina, C. M.; Lisal, M.; Siperstein, F. R.; Gubbins, K. E. *Fluid Phase Equilib.* **2002**, *202*, 253–262.
- (10) Lagache, M. H.; Ungerer, Ph.; Boutin, A.; Fuchs, A. H. *Phys. Chem. Chem. Phys.* **2001**, *3*, 4333–4339.
- (11) Lagache, M. H. *Fluid Phase Equilib.* **2004**, *220*, 211–223.
- (12) Colina, C. M.; Olivera-Fuentes, C. G.; Siperstein, F. R.; Lisal, M.; Gubbins, K. E. *Mol. Sim.* **2003**, *29* (6–7), 405–412.
- (13) Ungerer, P.; Tavittian, B.; Boutin, A. *Applications of molecular simulation in the oil and gas industry*; IFP publications, 2005.
- (14) Lisal, M.; Smith, W. R.; Aim, K. *Mol. Phys.* **2003**, *101*(18), 2875–2884.

- (15) Escobedo, F. A.; Chen, Z., *Mol. Simulation* **2001**, 26(6), 395–416.
- (16) Möller, D.; Oprzynski, J.; Müller, A. *Mol. Phys.* **1992**, 75, 363–378.
- (17) Allen, M. P.; Tildesley, D. J. *Computer Simulation of Liquids*; Oxford University Press: New York, 1987.
- (18) Frenkel, D.; Smit, B. *Understanding molecular simulation*; Academic Press: New York, 1996.
- (19) Randzio, S. L.; Grolier, J.-P. E.; Quint, J. R.; Eatough, D. J.; Lewis, E. A.; Hansen, L. D. *Int. J. Thermophys.* **1994**, 3, 415–441.
- (20) Gunn, R. D.; Chueh, P. L.; Prausnitz, J. M. *Cryogenics* **1966**, 6, 324–329.
- (21) Wagner, W.; de Reuck, K. M. In *METHANE International Thermodynamic Tables of the Fluid State*; International Union of Pure and Applied Chemistry; Blackwell Science: Oxford, 1996; vol. 13.
- (22) Setzmann, U.; Wagner W. *J. Phys. Chem. Ref data* **1991**, 20(6) 1061–1151.
- (23) Chapman, W. G.; Gubbins, K. E.; Jackson, G.; Radosz, M. *Ind. Eng. Chem. Res.* **1990**, 29, 1709–1721.
- (24) Gross, J.; Sadowski, G. *Ind. Eng. Chem. Res.* **2001**, 40, 1244–1260.
- (25) Gil-Villegas, A.; Galindo, A.; Whitehead, P. J.; Mills, S. J.; Jackson, G.; Burgess, A. N. *J. Chem. Phys.* **1997**, 106, 4168–4186